Hindawi
Mathematical Problems in Engineering
Volume 2018, Article ID 9487581, 10 pages
https://doi.org/10.1155/2018/9487581

Research Article

Steady-State Performance Analysis of Tracking Filter Using LFM Waveforms and Range-Rate Measurement

Kenshi Saho

Department of Intelligent Robotics, Toyama Prefectural University, Imizu 939-0398, Japan

Correspondence should be addressed to Kenshi Saho; saho@pu-toyama.ac.jp

Received 14 September 2018; Revised 9 November 2018; Accepted 21 November 2018; Published 4 December 2018

Academic Editor: Nazrul Islam

The steady-state performance of a moving-object tracking filter is theoretically analyzed, assuming the simultaneous measurement of the range and range-rate (RRM system), and the use of linear frequency modulated (LFM) waveforms (RRM-LFM filter). An efficient analytical steady-state performance index, called an RMS index, is derived for the RRM-LFM filter to clarify the steady-state range prediction errors, theoretically. Using the derived RMS index, the optimal performance of the RRM-LFM filter is analyzed. The performance variation due to the use of LFM waveforms is clarified for the RRM tracking system. The theoretical performance analysis verifies that the measured range-rate significantly improves the tracking accuracy, compared to the conventional range-only measuring LFM tracking filter. Furthermore, the quantitative relationships among the measurement accuracy, degree of target maneuvering, and steady-state range prediction errors are clarified to validate the effectiveness of the RRM-LFM filter.

1. Introduction

Tracking filters for robots and aircrafts predict the trajectory and velocity of a maneuvering target based on the measurements by remote sensors, such as radars, lidars, and/or sonars. For certain applications in such fields, linear frequency-modulated (LFM) waveforms are used for improving the resolution of the range measurements and imaging [1–4]. In measurements using LFM waveforms, a bias error occurs due to the Doppler effect, known as range-Doppler coupling [4, 5], which must be compensated. To reduce such bias errors, Kalman [6, 7] and α-β filters [8–10] modified for LFM waveforms are used. The analysis of the α-β filter for LFM waveforms (LFM α-β filter) is important because it theoretically clarifies the mathematical formulation of the steady-state performances of tracking filters [5, 9, 10]. Based on the theoretical performance analysis, an optimal tracking filter that minimizes the steady-state range prediction errors for LFM waveforms is derived and validated [8].

Most conventional studies on steady-state LFM tracking filters have considered the measurement of the range (distance) alone [5, 8–10], neglecting the measurement of the range-rate. However, owing to technical advancements, recent LFM radar systems can generally measure the range and range-rate with sufficient accuracy [1–4, 11]. In [4], a measurement model incorporating compensation for range-Doppler coupling using the measured range-rate was presented and applied to radar ship tracking. In addition, the effectiveness of this tracking technique was validated in various real environments [12, 13]. Therefore, the performance analysis of tracking filters for range-rate-measured (RRM) systems is important for their appropriate design [14–17]. Although Bar-Shalom [14] presented numerical examples of an LFM tracking filter for RRM measurement, a stringent theoretical analysis was not provided. Recently, some studies have clarified the performance of LFM radar tracking by numerical simulations [15–17]; however, their practicalities were confirmed only in limited situations. Hence, these studies have empirically designed the tracking-filter parameters, and the performance was not sufficiently investigated. In view of the above, a theoretical performance analysis of tracking filters for LFM waveforms, assuming an RRM system, is required for their appropriate design.

For the steady-state performance analysis of RRM systems, without using LFM waveforms, our previous work had proposed an efficient analytical performance index that

expresses the steady-state error in range prediction, called the root-mean-square index (RMS index) [8, 18]. We had presented an RMS index-based optimal design strategy for a steady-state second-order tracking filter using an RRM system, called the α-β-η-θ filter [18, 19]. Moreover, the previous research [8] had verified that the tracking accuracy of an LFM α-β filter designed using the RMS index is better than that designed using a representative Kalman-filter equation-based approach [9, 10]. Based on these studies, we believe that an RMS index-based analysis can reveal the theoretical performance and enable the optimal design of a steady-state tracking filter using an RRM system with LFM waveforms.

In this paper, the theoretical analysis of a tracking filter, using LFM waveforms and an RRM system (RRM-LFM filter), in steady-state is presented. The α-β-η-θ filter design [18] is extended to the use of LFM waveforms through the derivation of the RMS index. The derived RMS index-based analysis clarifies the relationship between the parameters of the LFM waveforms and the tracking accuracy of the RRM-LFM filter. The theoretical steady-state performance of the RRM-LFM filter is compared to that of the conventional LFM α-β and α-β-η-θ filters to reveal the effects of the use of LFM waveforms in an RRM system and demonstrate the effectiveness of range-rate measurement for tracking with LFM waveforms.

2. LFM Tracking Filter with Range-Rate Measurement

2.1. Problem Definition. This paper considers a steady-state second-order tracking filter using LFM waveforms, assuming the simultaneous measurement of the range and range-rate (RRM system). Figure 1 outlines a system for measurement using LFM waveforms and the tracking filter assumed in this study. First, a measurement model for the RRM system is described to define the tracking filter. This study assumes the measurement model presented in [4]. Moving-object tracking along the range direction using LFM waveforms is assumed, and the target state includes the range, r, and range-rate, v. At each time step k, the target range, r_{ok}, and the range-rate, v_{ok}, measured using LFM waveforms are input to the tracking filter. It is traditionally known that the range measured using the LFM waveforms includes not only the random errors due to sensor noise but also bias error due to the Doppler shift, which is modeled as [5]

$$r'_{ok} = r_{tk} + \Delta t v_{tk} + w_{rk}, \tag{1}$$

where r_{tk} and v_{tk} are the true range and range-rate at time kT, T is the sampling interval, w_{rk} is the white Gaussian noise in terms of the range with a standard deviation, σ_r, and Δt is the coefficient of the range-Doppler coupling expressed as [4, 5, 10]

$$\Delta t = \frac{\tau f_0}{B_w}, \tag{2}$$

where τ, f_0, and B_w are the pulse length, carrier frequency, and bandwidth of the LFM waveform, respectively. $\Delta t > 0$ corresponds to an up-chirp waveform, while $\Delta t < 0$ corresponds to a down-chirp one [5]. For the RRM system, the range-Doppler coupling, $\Delta t v_{tk}$, in the range measurement of (1) is compensated using the measured range-rate, v_{ok}, at each time step [4]. This compensation process is expressed as [4]

$$r_{ok} = r'_{ok} - \Delta t v_o = r_{tk} + \Delta t v_{tk} + w_{rk} - \Delta t v_{ok}. \tag{3}$$

We assume that the measured range-rate also contained the white Gaussian noise as [4]

$$v_{ok} = v_{tk} + w_{vk}, \tag{4}$$

where w_{vk} is the white Gaussian noise in terms of the range-rate with a standard deviation, σ_v. Substituting (4) into (3), we have

$$r_{ok} = r_{tk} + w_{rk} - \Delta t w_{vk}, \tag{5}$$

where w_{rk} and w_{vk} are independent. The measurement models of the RRM system for defining the filtering process are (4) and (5). As indicated in (5), although the bias error due to the Doppler shift is removed by the range-rate correction in (3), r_{ok} is affected by random errors in v_{ok} and the coefficient of the range-Doppler coupling. Thus, the reduction of these errors is required in the tracking filtering process.

From the measured parameters, r_{ok} and v_{ok}, the tracking filter calculates the predicted range, r_{pk}, and the range-rate, v_{pk}, as the outputs, as indicated in Figure 1. The tracking filter invokes an iterative prediction and smoothing process. The second-order tracking filter assumes a constant range-rate motion model for the prediction process, which is expressed as follows [8–10]:

$$r_{pk+1} = r_{sk} + T v_{sk}, \tag{6}$$

$$v_{pk+1} = v_{sk}, \tag{7}$$

where r_{pk} is the predicted target range, v_{pk} is the predicted target range-rate, and r_{sk} and v_{sk} are the smoothed range and range-rate, respectively, obtained in the smoothing process. The smoothing process of the RRM system is given by [18]

$$r_{sk} = r_{pk} + \alpha\left(r_{ok} - r_{pk}\right) + T\eta\left(v_{ok} - v_{pk}\right), \tag{8}$$

$$v_{sk} = v_{pk} + \left(\frac{\beta}{T}\right)\left(r_{ok} - r_{pk}\right) + \theta\left(v_{ok} - v_{pk}\right), \tag{9}$$

where α, β, η, and θ are the filter gains.

The aim of this paper is to clarify the steady-state performance of the tracking filter, expressed by (6)–(9), whose measurement models are (4) and (5). We refer to this tracking filter as the RRM-LFM filter. The assumptions made are as follows:

(i) The measurement parameters σ_r, σ_v, and Δt are known and constant.

(ii) The sampling interval, T, is known and constant.

(iii) As a steady-state is assumed, the filter gains α, β, η, and θ are fixed.

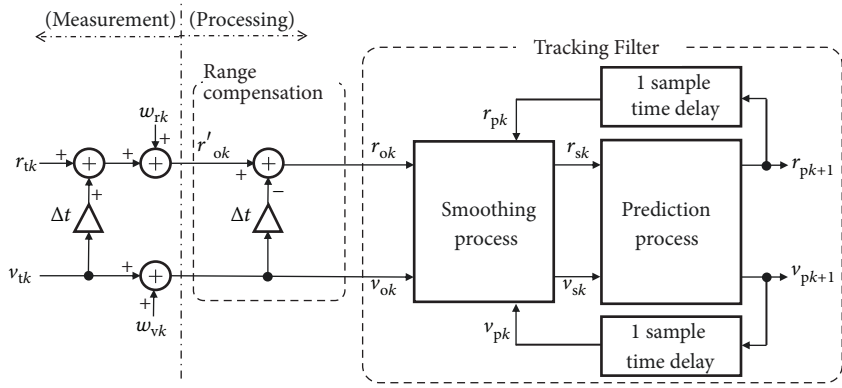

Figure 1: Outline of the assumed measurement/tracking system.

(iv) Filter gains that minimize the RMS index [8, 18] are set. The RMS index is a performance index of the tracking filter that expresses the mean of the steady-state errors in the predicted range.

In the rest of this paper, the RMS index of the RRM-LFM filter is derived. Then, the optimal gain is calculated using the derived RMS index. Finally, to clarify the effectiveness of the RRM-LFM filter, its optimal performance is compared with those of the conventional range-only measured LFM tracking filter (LFM α-β filter) [8–10] and the range and range-rate measured filter without considering LFM waveforms (α-β-η-θ filter) [18].

2.2. Relationship with the LFM α-β Filter. The LFM α-β filter is a steady-state tracking filter for LFM waveforms, assuming a range only measurement [8–10]. The difference between the LFM α-β and RRM-LFM filters is that the measurement range-rate, v_o, is not obtained in the former. Thus, differing from (3), the range-Doppler coupling is not compensated in the measurement process. Instead, this is compensated in the smoothing process of the tracking filter. The smoothing process in the LFM α-β filter is given by [8–10]

$$r_{sk} = r_{pk} + \alpha\left(r_{ok} - \Delta t v_{pk} - r_{pk}\right), \tag{10}$$

$$v_{sk} = v_{pk} + \left(\frac{\beta}{T}\right)\left(r_{ok} - \Delta t v_{pk} - r_{pk}\right). \tag{11}$$

The prediction process is the same as (6) and (7). As indicated in (10) and (11), the bias error due to range-Doppler coupling in r_o is compensated using the predicted range-rate, v_p. The optimization of the LFM α-β filter is presented in [10]. The comparison of the RRM-LFM and LFM α-β filters reveals the effectiveness of range-rate measurements in LFM radars.

2.3. Relationship with the α-β-η-θ Filter. The α-β-η-θ filter is a steady-state tracking filter, which considers the range and range-rate (position and velocity) measurements [18, 19]. The filtering process is the same as that of the RRM-LFM filter, i.e., (6)–(9). Although its performance analysis and optimization are presented in [18], the use of LFM waveforms is not considered. The conventional performance analysis of the α-β-η-θ filter assumes that there is no error covariance between the range and range-rate. The variances and covariance of the measurement noise assumed in [18] are as follows:

$$\begin{aligned} \mathrm{E}\left[\left(r_{ok}^{\mathrm{conv}} - r_{tk}\right)^2\right] &= \sigma_r^2, \\ \mathrm{E}\left[\left(v_{ok}^{\mathrm{conv}} - v_{tk}\right)^2\right] &= \sigma_v^2, \\ \mathrm{E}\left[\left(r_{ok}^{\mathrm{conv}} - r_{tk}\right)\left(v_{ok}^{\mathrm{conv}} - v_{tk}\right)\right] &= 0, \end{aligned} \tag{12}$$

where E[ ] indicates the mean with respect to k and r_o^{conv} and v_o^{conv} are the measurement range and range-rate, respectively, assumed in conventional studies. The performance analysis and design of the optimal filter gains of the α-β-η-θ filter assume (12). However, for the RRM-LFM filter, the error covariances of r_o and v_o apparently exist, as indicated in (5). Thus, the analysis of the filter expressed by (6)–(9), considering the error covariance matrix of the measurements expressed by (4) and (5), is required for determining its performance. The comparison of the RRM-LFM and conventional α-β-η-θ filters reveals the effect of range-Doppler coupling on the RRM system.

3. Performance Index and Optimal Gain of the RRM-LFM Filter

This section derives the RMS index of the RRM-LFM filter in a closed form and presents the optimal calculation procedure for the filter gains. The definition of the RMS-index is given by [8]

$$\varepsilon_p \equiv \lim_{k\longrightarrow\infty}\sqrt{\mathrm{E}\left[\left(r_{tk}^{\mathrm{ca}} - r_{pk}\right)^2\right]} = \sqrt{\sigma_p^2 + \left(L_{rp}A_{\max}T^2\right)^2}, \tag{13}$$

where

$$r_{tk}^{\mathrm{ca}} = \frac{A_{\max}(kT)^2}{2} \tag{14}$$

is the true range of a target moving at constant acceleration, $A_{\max}$; σ_p^2 is the steady-state error variance in the range prediction assuming only sensor noise; and $L_{rp}A_{\max}T^2$ is the steady-state bias error in the range prediction [8, 10]. σ_p^2 expresses the degree of random error due to sensor noise, and

$L_{\mathrm{rp}}A_{\max}T^2$ is the bias error caused by the difference between the assumed motion model (constant-range-rate model or constant-velocity model) and the target motion (accelerating motion). When we assume that the maximum acceleration of the target is $A_{\max}$, the RMS index expresses the maximum RMS error of the range prediction in steady-state, for the second-order tracking filter (a detailed discussion is available in [18]).

The optimal filter gains are calculated by the minimization of ε_{p}. Thus, we need σ_{p}^2 and L_{rp} to derive ε_{p} of the RRM-LFM filter. Moreover, to derive σ_{p}^2, the variances and covariance of the measurement errors in the RRM system are required. Thus, in the following subsections, the variances and covariance of the measurement errors are derived. Using these, σ_{p}^2 is derived. Further, L_{rp} and ε_{p} are determined, and the optimal gain calculation procedure is finally presented.

3.1. Derivation of the Measurement Error Variance/Covariance. In this section, the covariance matrix of the RRM-LFM filter is derived for the derivation of the RMS index. With (4) and (5), the measurement errors at time, kT, are

$$r_{ok} - r_{tk} = w_{rk} - \Delta t w_{vk}, \tag{15}$$

$$v_{ok} - v_{tk} = w_{vk}. \tag{16}$$

Using (15) and (16), the variances and covariance of these errors are calculated as follows:

$$\begin{aligned}\sigma_{\mathrm{ro}}^2 &\equiv E\left[\left(r_{ok} - r_{tk}\right)^2\right] \\ &= \Delta t^2 \mathrm{E}\left[w_{vk}^2\right] + \mathrm{E}\left[w_{rk}^2\right] + 2\Delta t \mathrm{E}\left[w_{vk} w_{rk}\right] \\ &= \Delta t^2 \sigma_{\mathrm{v}}^2 + \sigma_{\mathrm{r}}^2,\end{aligned} \tag{17}$$

$$\sigma_{\mathrm{vo}}^2 \equiv \mathrm{E}\left[\left(v_{ok} - v_{tk}\right)^2\right] = \mathrm{E}\left[w_{vk}^2\right] = \sigma_{\mathrm{v}}^2, \tag{18}$$

$$\begin{aligned}\sigma_{x\mathrm{vo}}^2 &\equiv \mathrm{E}\left[\left(r_{ok} - r_{tk}\right)\left(v_{ok} - v_{tk}\right)\right] \\ &= -\Delta t \mathrm{E}\left[w_{vk}^2\right] + E\left[w_{vk} w_{rk}\right] = -\Delta t \sigma_{\mathrm{v}}^2.\end{aligned} \tag{19}$$

3.2. Derivation of the Range Prediction Steady-State Error Variance. σ_{p}^2 is defined as [8, 18]

$$\sigma_{\mathrm{p}}^2 \equiv \lim_{k \longrightarrow \infty} \mathrm{E}\left[\left(r_{tk}^{\mathrm{cv}} - r_{pk}\right)^2\right], \tag{20}$$

where r_{tk}^{cv} is the true range of a target moving at a constant range-rate. Because the RRM-LFM filter assumes a constant range-rate model, random errors due to sensor noise alone are included in the predicted range of the target moving at a constant range-rate. Thus, the true target motion for the derivation of σ_{p}^2 is the constant range-rate motion.

σ_{p}^2 of the RRM-LFM filter is derived as follows. r_{tk}^{cv} can be expressed as

$$r_{tk}^{\mathrm{cv}} = r_{tk-1}^{\mathrm{cv}} + T v_{\mathrm{t}}^{\mathrm{cv}}. \tag{21}$$

With (6) and (21), the mean squared predicted error is calculated as

$$\begin{aligned}&\mathrm{E}\left[\left(r_{tk}^{\mathrm{cv}} - r_{pk}\right)^2\right] \\ &\quad = \mathrm{E}\left[\left(r_{tk-1}^{\mathrm{cv}} - r_{sk-1}\right)^2\right] \\ &\qquad + 2T\mathrm{E}\left[\left(r_{tk-1}^{\mathrm{cv}} - r_{sk-1}\right)\left(v_{\mathrm{t}}^{\mathrm{cv}} - v_{\mathrm{sk}-1}\right)\right] \\ &\qquad + \mathrm{E}\left[\left(v_{\mathrm{t}}^{\mathrm{cv}} - v_{\mathrm{sk}-1}\right)^2\right].\end{aligned} \tag{22}$$

Because we assume a steady-state ($k \longrightarrow \infty$), we can define following smoothing error variance/covariance:

$$\sigma_{\mathrm{rs}}^2 \equiv \mathrm{E}\left[\left(r_{tk-1}^{\mathrm{cv}} - r_{sk-1}\right)^2\right] = \mathrm{E}\left[\left(r_{tk}^{\mathrm{cv}} - r_{sk}\right)^2\right], \tag{23}$$

$$\begin{aligned}\sigma_{\mathrm{rvs}}^2 &\equiv \mathrm{E}\left[\left(r_{tk-1}^{\mathrm{cv}} - r_{sk-1}\right)\left(v_{\mathrm{t}}^{\mathrm{cv}} - v_{sk-1}\right)\right] \\ &= \mathrm{E}\left[\left(r_{tk}^{\mathrm{cv}} - r_{sk}\right)\left(v_{\mathrm{t}}^{\mathrm{cv}} - v_{sk}\right)\right],\end{aligned} \tag{24}$$

$$\sigma_{\mathrm{vs}}^2 \equiv \mathrm{E}\left[\left(v_{\mathrm{t}}^{\mathrm{cv}} - v_{sk-1}\right)^2\right] = \mathrm{E}\left[\left(v_{\mathrm{t}}^{\mathrm{cv}} - v_{sk}\right)^2\right]. \tag{25}$$

With (20) and (22)–(25),

$$\sigma_{\mathrm{p}}^2 = \sigma_{\mathrm{xs}}^2 + 2T\sigma_{\mathrm{xvs}}^2 + T^2\sigma_{\mathrm{vs}}^2. \tag{26}$$

Therefore, σ_{xs}^2, σ_{xvs}^2, and σ_{vs}^2 are then derived to calculate (26). The true range and range-rate can be expressed similar to (8) and (9) as

$$r_{tk}^{\mathrm{cv}} = r_{tk}^{\mathrm{cv}} + \alpha\left(r_{tk}^{\mathrm{cv}} - r_{tk}^{\mathrm{cv}}\right) + T\eta\left(v_{\mathrm{t}}^{\mathrm{cv}} - v_{\mathrm{t}}^{\mathrm{cv}}\right), \tag{27}$$

$$v_{\mathrm{t}}^{\mathrm{cv}} = v_{\mathrm{t}}^{\mathrm{cv}} + \left(\frac{\beta}{T}\right)\left(r_{tk}^{\mathrm{cv}} - r_{tk}^{\mathrm{cv}}\right) + \theta\left(v_{\mathrm{t}}^{\mathrm{cv}} - v_{\mathrm{t}}^{\mathrm{cv}}\right). \tag{28}$$

The smoothing errors are calculated using (8), (9), (27), and (28) as

$$\begin{aligned}r_{tk}^{\mathrm{cv}} - r_{sk} &= (1-\alpha)\left(r_{tk}^{\mathrm{cv}} - r_{pk}\right) + \alpha\left(r_{tk}^{\mathrm{cv}} - r_{ok}\right) \\ &\quad + T\eta\left\{\left(v_{\mathrm{t}}^{\mathrm{cv}} - v_{ok}\right) - \left(v_{\mathrm{t}}^{\mathrm{cv}} - v_{pk}\right)\right\},\end{aligned} \tag{29}$$

$$\begin{aligned}v_t^{cv} - v_{sk} &= (1-\theta)\left(v_t^{cv} - v_{pk}\right) + \theta\left(v_t^{cv} - v_{ok}\right) \\ &\quad + \left(\frac{\beta}{T}\right)\left\{\left(r_{tk}^{cv} - r_{ok}\right) - \left(r_{tk}^{cv} - r_{pk}\right)\right\}.\end{aligned} \tag{30}$$

Substituting (6), (7), and (21) into (29) and (30),

$$\begin{aligned}r_{tk}^{\mathrm{cv}} - r_{sk} &= (1-\alpha)\left\{\left(r_{tk-1}^{\mathrm{cv}} - r_{sk-1}\right) + T\left(v_{\mathrm{t}}^{\mathrm{cv}} - v_{sk-1}\right)\right\} \\ &\quad + \alpha\left(r_{tk}^{\mathrm{cv}} - r_{ok}\right) + T\eta\left\{\left(v_{\mathrm{t}}^{\mathrm{cv}} - v_{ok}\right) - \left(v_{\mathrm{t}}^{\mathrm{cv}} - v_{sk-1}\right)\right\},\end{aligned} \tag{31}$$

$$\begin{aligned}v_{\mathrm{t}}^{\mathrm{cv}} - v_{sk} &= (1-\theta)\left(v_{\mathrm{t}}^{\mathrm{cv}} - v_{sk-1}\right) + \theta\left(v_{\mathrm{t}}^{\mathrm{cv}} - v_{ok}\right) \\ &\quad + \left(\frac{\beta}{T}\right) \\ &\quad \cdot \left\{\left(r_{tk}^{\mathrm{cv}} - r_{ok}\right) - \left(r_{tk-1}^{\mathrm{cv}} - r_{sk-1}\right) - T\left(v_{\mathrm{t}}^{\mathrm{cv}} - v_{sk-1}\right)\right\}.\end{aligned} \tag{32}$$

Using (31), the error variance of the smoothed range is calculated as

$$\begin{aligned}
\mathrm{E}\left[\left(r_{tk}^{cv}-r_{sk}\right)^2\right] &= (1-\alpha)^2\left\{\mathrm{E}\left[\left(r_{tk-1}^{cv}-r_{sk-1}\right)^2\right]\right.\\
&+T^2\mathrm{E}\left[\left(v_t^{cv}-v_{sk-1}\right)^2\right]\\
&\left.+2T\mathrm{E}\left[\left(r_{tk-1}^{cv}-r_{sk-1}\right)\left(v_t^{cv}-v_{sk-1}\right)\right]\right\}\\
&+\alpha^2\mathrm{E}\left[\left(r_{tk}^{cv}-r_{ok}\right)^2\right]+T^2\eta^2\left\{\mathrm{E}\left[\left(v_t^{cv}-v_{ok}\right)^2\right]\right.\\
&-\mathrm{E}\left[\left(v_t^{cv}-v_{sk-1}\right)^2\right]\\
&\left.-2T\mathrm{E}\left[\left(v_t^{cv}-v_{ok}\right)\left(v_t^{cv}-v_{sk-1}\right)\right]\right\}+2\alpha(1-\alpha)\\
&\cdot\left\{\mathrm{E}\left[\left(r_{tk-1}^{cv}-r_{sk-1}\right)\left(r_{tk}^{cv}-r_{ok}\right)\right]\right.\\
&\left.+T\mathrm{E}\left[\left(v_t^{cv}-v_{sk-1}\right)\left(r_{tk}^{cv}-r_{ok}\right)\right]\right\}\\
&+2T\alpha\eta\left\{\mathrm{E}\left[\left(r_{tk}^{cv}-r_{ok}\right)\left(v_t^{cv}-v_{ok}\right)\right]\right.\\
&\left.-\mathrm{E}\left[\left(r_{tk}^{cv}-r_{ok}\right)\left(v_t^{cv}-v_{sk-1}\right)\right]\right\}+2T\eta(1-\alpha)\\
&\cdot\left\{\mathrm{E}\left[\left(r_{tk-1}^{cv}-r_{sk-1}\right)\left(v_t^{cv}-v_{ok}\right)\right]\right.\\
&-\mathrm{E}\left[\left(r_{tk}^{cv}-r_{sk-1}\right)\left(v_t^{cv}-v_{sk-1}\right)\right]\\
&+T\mathrm{E}\left[\left(v_t^{cv}-v_{sk-1}\right)\left(v_t^{cv}-v_{ok}\right)\right]\\
&\left.-T\mathrm{E}\left[\left(v_t^{cv}-v_{sk-1}\right)^2\right]\right\}.
\end{aligned} \tag{33}$$

The following relations are satisfied because the smoothed parameters are a linear combination of the measured parameters:

$$\begin{aligned}
\mathrm{E}\left[\left(r_{tk-1}^{cv}-r_{sk-1}\right)\left(r_{tk}^{cv}-r_{ok}\right)\right]&=0,\\
\mathrm{E}\left[\left(v_t^{cv}-v_{ok}\right)\left(v_t^{cv}-v_{sk-1}\right)\right]&=0,\\
\mathrm{E}\left[\left(v_t^{cv}-v_{sk-1}\right)\left(r_{tk}^{cv}-r_{ok}\right)\right]&=0,\\
\mathrm{E}\left[\left(r_{tk-1}^{cv}-r_{sk-1}\right)\left(v_t^{cv}-v_{ok}\right)\right]&=0.
\end{aligned} \tag{34}$$

Substituting (17)–(19), (23)–(25), and (34) into (33), and simplifying, we obtain a linear equation with respect to σ_{xs}^2, σ_{xvs}^2, and σ_{vs}^2 as

$$\begin{aligned}
&\alpha(2-\alpha)\sigma_{xs}^2+2(1-\alpha)(\alpha+\eta-1)T\sigma_{xvs}^2\\
&-(\alpha+\eta-1)^2T^2\sigma_{vs}^2=\alpha^2\sigma_r^2+(\eta T-\alpha\Delta t)^2\sigma_v^2.
\end{aligned} \tag{35}$$

Similar to the above calculation of $\mathrm{E}[(r_{tk}^{cv}-r_{sk})^2]$ using (32), we obtain another linear equation from the calculation of $\mathrm{E}[(v_t^{cv}-v_{sk})^2]$ as

$$\begin{aligned}
&-\beta^2\sigma_{xs}^2+2\beta(1-\beta-\theta)T\sigma_{xvs}^2\\
&+(2-\beta-\theta)(\beta+\theta)T^2\sigma_{vs}^2\\
&=\beta^2\sigma_r^2+(\theta T-\beta\Delta t)^2\sigma_v^2.
\end{aligned} \tag{36}$$

With the calculation of $\mathrm{E}[(r_{tk}^{cv}-r_{sk})(v_t^{cv}-v_{sk})]$ using (29) and (30), we also have

$$\begin{aligned}
&\beta(1-\alpha)\sigma_{xs}^2+(\alpha+2\beta+\theta-\alpha\theta-\beta\eta-2\alpha\beta)T\sigma_{xvs}^2\\
&+(\alpha+\eta-1)(1-\beta-\theta)T^2\sigma_{vs}^2\\
&=\alpha\beta\sigma_r^2+(\eta T-\alpha\Delta t)(\theta T-\beta\Delta t)\sigma_v^2.
\end{aligned} \tag{37}$$

Substituting the solution (σ_{xs}^2, σ_{xvs}^2, σ_{vs}^2) of the linear system composed of (35)–(37) into (26), we arrive at σ_p^2 as

$$\sigma_p^2=\frac{g_2(\alpha,\beta,\eta,\theta)\sigma_r^2+\left\{T^2g_3(\alpha,\beta,\eta,\theta)+2T\Delta tg_4(\alpha,\beta,\eta,\theta)+\Delta t^2g_2(\alpha,\beta,\eta,\theta)\right\}\sigma_v^2}{g_1(\alpha,\beta,\eta,\theta)}, \tag{38}$$

where

$$g_1(\alpha,\beta,\eta,\theta)=(\alpha+\theta+\beta\eta-\alpha\theta)(4-2\alpha-\beta-2\theta+\alpha\theta-\beta\eta), \tag{39}$$

$$g_2(\alpha,\beta,\eta,\theta)=\alpha^2\theta^2-\alpha\theta^2-2\alpha\beta\eta\theta+\beta\eta\theta-\alpha\beta\theta-\beta\theta-3\alpha^2\theta+2\alpha\theta+\beta^2\eta^2+\beta^2\eta+3\alpha\beta\eta-2\beta\eta+\alpha\beta+2\beta+2\alpha^2, \tag{40}$$

$$g_3(\alpha,\beta,\eta,\theta)=\frac{\left(\alpha^2\theta^3-\theta^3-\beta\eta\theta^2+2\alpha\eta\theta^2-\alpha\theta^2+2\theta^2-2\beta\eta^2\theta+2\alpha\eta^2\theta+2\beta\eta\theta-2\beta\eta^3+2\beta\eta^2\right)}{(\alpha\theta-\beta\eta+\beta)}, \tag{41}$$

$$g_4(\alpha,\beta,\eta,\theta)=\theta^2+\alpha\eta\theta-2\theta-\beta\eta^2-\beta\eta-2\alpha\eta. \tag{42}$$

Note that, when $\Delta t = 0$, σ_p^2 of (38) is equal to the steady-state error variance of the predicted position in the conventional α-β-η-θ filter presented in [18], which does not consider range-Doppler coupling.

3.3. Derivation of the RMS Index. The coefficient L_{rp} is also required for deriving the RMS index. However, this is equivalent to that of the conventional α-β-η-θ filter. This is because it is assumed that there are no random errors in the derivation of L_{rp} [18], and the bias error due to Δt is completely compensated by v_o in this situation, as indicated in (1). Thus, L_{rp} is (see Eq. (26) of [18])

$$L_{rp} = \frac{2 - 2\eta - \theta}{2(\alpha\theta - \beta\eta + \beta)}. \tag{43}$$

The RMS index of the RRM-LFM filter is derived by substituting (38) and (43) into (13) as

$$\varepsilon_p = \left\{ \frac{g_2(\alpha,\beta,\eta,\theta)\sigma_r^2 + \left\{T^2 g_3(\alpha,\beta,\eta,\theta) + 2T\Delta t g_4(\alpha,\beta,\eta,\theta) + \Delta t^2 g_2(\alpha,\beta,\eta,\theta)\right\}\sigma_v^2}{g_1(\alpha,\beta,\eta,\theta)} + \left(\frac{2 - 2\eta - \theta}{2(\alpha\theta - \beta\eta + \beta)}\right)^2 A_{max}^2 T^4 \right\}^{1/2}. \tag{44}$$

Table 1 summarizes the features and RMS indices of the tracking filters, whose steady-state performances are analyzed in Section 4.

3.4. Optimal Gain Calculation. The optimal gains are calculated by minimizing the RMS index. Based on (44), an evaluating function is defined as

$$\begin{aligned}\mu(\alpha,\beta,\eta,\theta,R_{rv},c_{RD},\Gamma_D) &\equiv \frac{\varepsilon_p^2}{T^2\sigma_v^2} \\ &= \frac{g_2(\alpha,\beta,\eta,\theta)R_{rv} + g_3(\alpha,\beta,\eta,\theta) + 2c_{RD}g_4(\alpha,\beta,\eta,\theta) + c_{RD}^2 g_2(\alpha,\beta,\eta,\theta)}{g_1(\alpha,\beta,\eta,\theta)} \\ &\quad + \left(\frac{2 - 2\eta - \theta}{2(\alpha\theta - \beta\eta + \beta)}\right)^2 R_{rv}\Gamma_D^2,\end{aligned} \tag{45}$$

where

$$R_{rv} \equiv \frac{\sigma_r^2}{(T^2\sigma_v^2)} \tag{46}$$

indicates the ratio of the measurement accuracies in the range and range-rate [18];

$$c_{RD} \equiv \frac{\Delta t}{T} \tag{47}$$

is the normalized coefficient of the range-Doppler coupling [5]; and

$$\Gamma_D \equiv \frac{A_{max}T^2}{\sigma_r} \tag{48}$$

is the deterministic tracking index defined in [10]. Γ_D indicates the degree of maneuvering of the target. The optimal gains of the RRM-LFM filter are obtained by solving the following problem:

$$\begin{aligned}&\arg\min_{\alpha,\beta,\eta,\theta} && \mu(\alpha,\beta,\eta,\theta,R_{rv},c_{RD},\Gamma_D) \\ &\text{sub. to} && (1-\eta)\beta + \alpha\theta > 0 \text{ and} \\ &&& 4 - 2\alpha - \beta - 2\theta + \alpha\theta - \beta\eta > 0 \text{ and} \\ &&& |\alpha\theta - \beta\eta - \alpha - \theta + 1| < 1,\end{aligned} \tag{49}$$

where the constraints are the stability conditions of the α-β-η-θ filter [18].

4. Performance Analysis

4.1. Analysis Method. The minimum RMS index of the RRM-LFM, conventional α-β-η-θ, and LFM α-β filters are evaluated and compared by theoretical analyses. The minimization in (49) is solved by a simple gradient descent method, and the minimum RMS index, $\varepsilon_{p,min}$, is obtained by substituting the solutions of (49) into (44). $\varepsilon_{p,min}$ of the other conventional filters are similarly calculated, using their RMS indices (see Table 1). We assume that σ_r and T are normalized to unity and A_{max} is known. Varying R_{rv}, c_{RD}, and Γ_D, the performance

Table 1: Summary of the tracking filters considered in this paper.

Filter	Measurement parameter	LFM waveform	RMS index
LFM α-β	Range	Yes	See Eq. (17) of [8]
Conventional α-β-η-θ	Range and range rate	No	Eq. (44), when $\Delta t = 0$
Proposed RRM-LFM		Yes	Eq. (44)

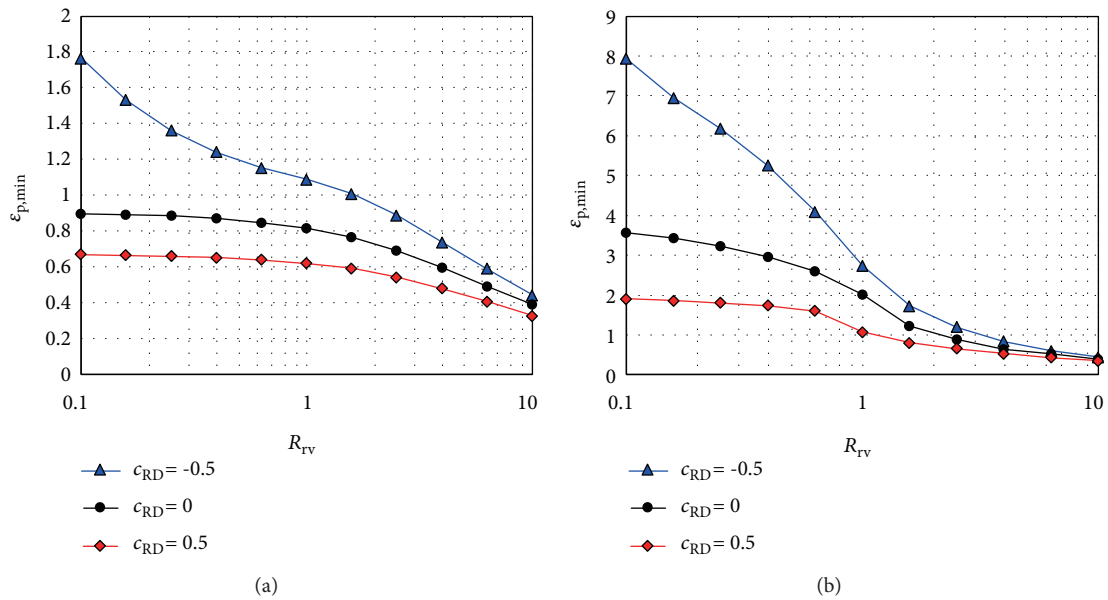

Figure 2: Relationship between R_{rv} and $\varepsilon_{p,min}$ for c_{RD} = -0.5, 0, 0.5: (a) Γ_D = 0.1. (b) Γ_D = 1.

is analyzed to quantitatively investigate the effect of range-Doppler coupling in the RRM system and the performance improvement by the application of the measured range-rate in LFM radar tracking.

4.2. Results and Discussion. Figure 2 shows the analysis results of the relationship between R_{rv} and $\varepsilon_{p,min}$ for c_{RD} = -0.5 (down-chirp), 0 (conventional α-β-η-θ filter without LFM waveforms), and 0.5 (up-chirp); Γ_D = 0.1 and 1. As shown in these results, a larger R_{rv} improves the steady-state tracking accuracy. On comparing the results for c_{RD}= 0.5 and 0, the improvement in the tracking accuracy by use of the up-chirp is confirmed. Although this improvement is known for range-only measured tracking systems [5], these results confirm a similar improvement in the RRM system, as well. As indicated in Figure 2(b), the performance improvement by using the up-chirp becomes considerable, when R_{rv} is small and Γ_D = 1. This establishes that the use of the up-chirp achieves accurate tracking, even when the target maneuvering is relatively large and the measurement accuracy of the range-rate is worse. In contrast, the performance deterioration due to the use of the down-chirp is also confirmed. When R_{rv} becomes small, indicating that the accuracy of the range-rate measurement is worse, the performance deterioration for c_{RD} = -0.5, compared to the results for c_{RD}= 0, becomes considerable. Moreover, by comparing the results in Figures 2(a) and 2(b), the deterioration of the tracking accuracy for c_{RD} = -0.5 is relatively large for Γ_D=1. These results indicate that the down-chirp significantly deteriorates the tracking accuracy, when the range-rate measurement is unreliable, and the accelerating motion of the target is relatively large. In contrast, as indicated by the results for a relatively large R_{rv}, the tracking accuracy depending on c_{RD} becomes small. This is because the compensation of the bias-error due to range-Doppler coupling is correctly performed in (3) by using a sufficiently accurate v_o (sufficiently small σ_v).

Figure 3 shows the analysis results of the relationship between c_{RD} and $\varepsilon_{p,min}$ for the LFM α-β and RRM-LFM filters with R_{rv} = 0.1, 1, and 10 and Γ_D = 0.1 and 1. The results for R_{rv} = 1 and 10 clearly indicate the enhancement of the steady-state tracking accuracy by using range-rate measurements. However, the results for R_{rv} = 0.1 at c_{RD} <0 and Γ_D = 0.1 demonstrate that the performance of the RRM-LFM filter is worse than that of the LFM α-β filter. This is because the compensation of the bias error in (3) is not accurate due to the poorer accuracy of the range-rate measurements. The LFM α-β filter compensates such errors using the estimated range-rate acquired in the filtering process, as indicated in (10) and (11). Moreover, errors due to the down-chirp also occur for c_{RD} < 0, and these are also not sufficiently suppressed in the RRM system. Furthermore, when Γ_D is small, the effects of a smaller R_{rv} and c_{RD} for the minimization of the RMS index become considerable because the first term of (38) becomes relatively large. Thus, there are cases where the performance

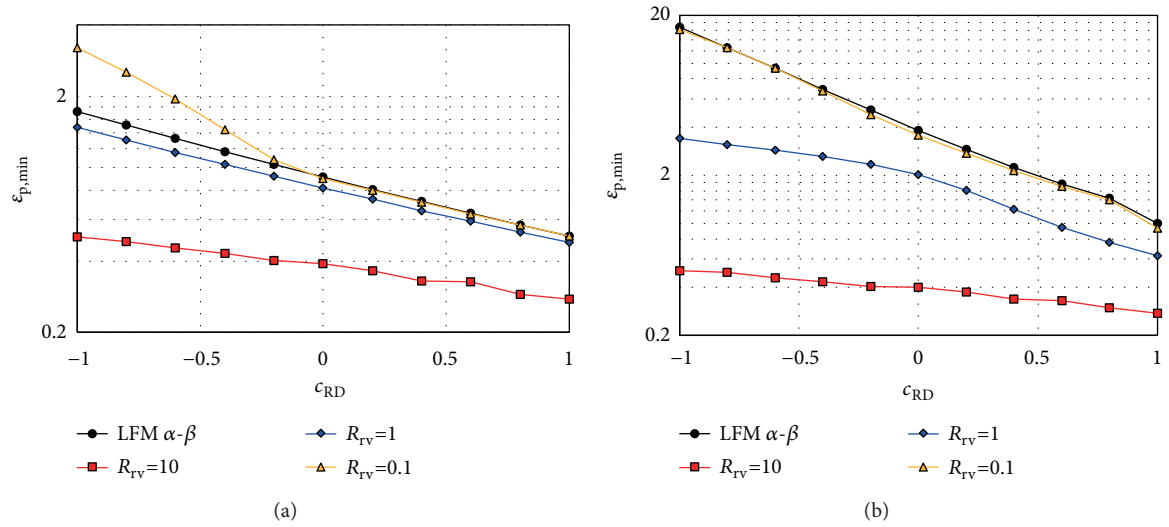

FIGURE 3: Relationship between c_{RD} and $\varepsilon_{p,min}$ of the LFM α-β and RRM-LFM filters with R_{rv} = 0.1, 1, and 10: (a) Γ_D = 0.1. (b) Γ_D = 1.

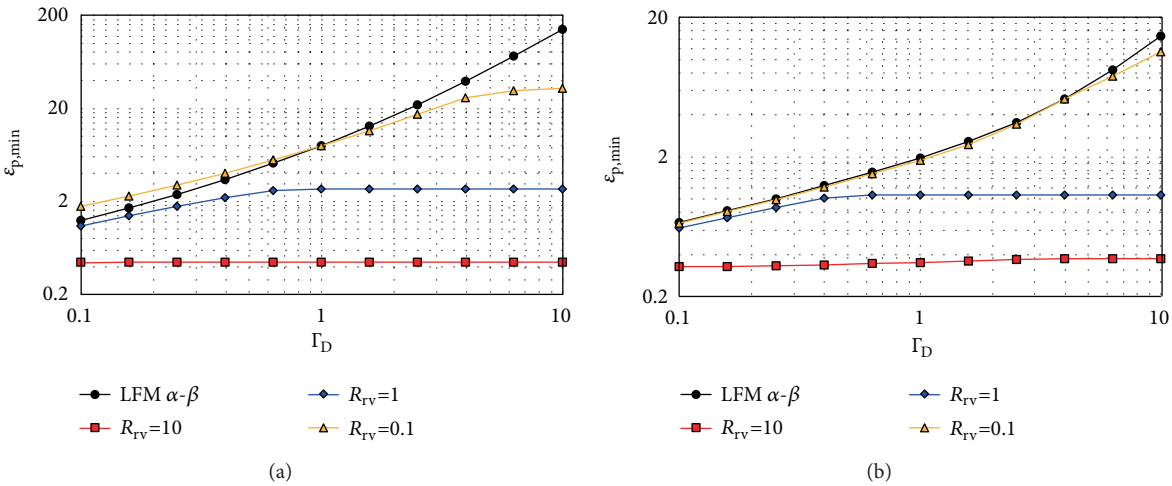

FIGURE 4: Relationship between Γ_D and $\varepsilon_{p,min}$ of the LFM α-β and RRM-LFM filters with R_{rv} = 0.1, 1, and 10: (a) c_{RD}= 0.5. (b) c_{RD}= -0.5.

of the RRM-LFM filter is worse than that of the range-only measured LFM α-β filter. This is a notable result because accuracy deterioration due to range-rate measurements does not occur in the conventional α-β-η-θ filter as proved in [18].

Figure 4 shows the analysis results of relationship between Γ_D and $\varepsilon_{p,min}$ for R_{rv} = 0.1, 1, and 10 and c_{RD} = -0.5 and 0.5. Although the errors in the LFM α-β filter deteriorate the tracking accuracy with the increase in Γ_D, those in the RRM-LFM filter converge because the RRM system effectively compensates the bias error using accurate range-rate information, when R_{rv} is relatively large. However, we can confirm that the tracking accuracy for R_{rv} = 0.1 is similar to that of the LFM α-β filter, when c_{RD} = 0.5 because the range-rate measurement accuracy is insufficient for improving the tracking accuracy. On the other hand, the RRM-LFM filter with R_{rv} = 0.1 and c_{RD} = -0.5 improves the accuracy for a relatively large Γ_D because the measured range-rate (or velocity) information is effectively used to compensate the bias errors due to target acceleration. It is relatively difficult for a range-only measured system to compensate the errors due to acceleration because acceleration is the second-derivative of the range. In addition, the performance of the RRM-LFM filter is worse than that of the LFM α-β filter for relatively small Γ_D, as discussed in the previous paragraph.

The summary of the analyses results is as follows. All the analysis results prove that the steady-state performance improvement is significant on using an RRM system for tracking with LFM waveforms, when the measurement accuracy of the range-rate is sufficiently large. Even for R_{rv}=1, when the reliabilities of the range and range-rate measurements are the same, the LFM tracking performance is improved. Furthermore, the effects of range-Doppler coupling and its compensation in the RRM system are quantitatively clarified. It is also revealed that there are cases where the performance of the RRM-LFM filter is worse than that of the conventional range-only measured LFM α-β filter, when down-chirp is used (c_{RD} < 0), and R_{rv} and Γ_D are

both relatively small. However, for real applications of RRM-LFM radars, this might not be a serious problem due to the following reasons:

(i) For applications, assuming relatively small range measurements, whose order is smaller than 10 m, such as intelligent vehicles, moving robots, and indoor surveillance systems, the sampling interval, T, is less than order of 100 ms. Thus, for such applications, R_{rv} becomes large, as indicated in (46).

(ii) For applications, assuming relatively large range measurements, whose order is greater than 100 m, such as aircraft tracking, the assumed maximum target acceleration, $A_{\max}$, and T are large. Thus, Γ_{D} becomes large.

Therefore, the representative applications of LFM radars do not consider a parameter setting, where Γ_{D} and R_{rv} are both small.

5. Conclusions

A range tracking filter using LFM waveforms and an RRM system was presented in this paper. The RMS index, which is a performance index that expresses the steady-state range prediction error, was analytically derived for the RRM-LFM filter, and its optimal gain, which minimizes the RMS index, was determined. The optimal steady-state performance of the RRM-LFM filter and its relationship with the measurement accuracy and range-Doppler coupling coefficient were theoretically analyzed. Performance comparison with the LFM α-β filter revealed the effectiveness of range-rate measurement quantitatively. Furthermore, the comparison of the RRM-LFM filter with the conventional α-β-η-θ filter clarified the effect of using LFM waveforms in an RRM system. Thus, it was established that range-rate measurement with sufficient accuracy significantly improves tracking accuracy with LFM waveforms.

Data Availability

The data used to support the findings of this study are available from the corresponding author upon request.

Conflicts of Interest

The author declares no conflicts of interest.

Acknowledgments

The author would like to thank Editage (https://www.editage.jp/) for English language editing. This work was supported in part by the JSPS KAKENHI [16K16093].

References

[1] J. Zhu, X. Wang, X. Huang, S. Suvorova, and B. Moran, "Detection of moving targets in sea clutter using complementary waveforms," *Signal Processing*, vol. 146, pp. 15–21, 2018.

[2] M. A. B. Othman, J. Belz, and B. Farhang-Boroujeny, "Performance Analysis of Matched Filter Bank for Detection of Linear Frequency Modulated Chirp Signals," *IEEE Transactions on Aerospace and Electronic Systems*, vol. 53, no. 1, pp. 41–54, 2017.

[3] F Wang, D Jiang, and H Chen, "High Range Resolution Profile Construction Exploiting Modified Fractional Fourier Transformation," *Mathematical Problems in Engineering*, vol. 2015, Article ID 321878, 11 pages, 2015.

[4] L. Bruno, P. Braca, J. Horstmann, and M. Vespe, "Experimental evaluation of the range-doppler coupling on HF surface wave radars," *IEEE Geoscience and Remote Sensing Letters*, vol. 10, no. 4, pp. 850–854, 2013.

[5] R. J. Fitzgerald, "Effects of Range-Doppler Coupling on Chirp Radar Tracking Accuracy," *IEEE Transactions on Aerospace and Electronic Systems*, vol. 10, no. 4, pp. 528–532, 1974.

[6] B. Wang, J. Sun, X. Zhang, and X. Yang, "A waveform-agile unscented Kalman filter for radar target tracking," in *Proceedings of the 9th International Congress on Image and Signal Processing, BioMedical Engineering and Informatics, CISP-BMEI 2016*, pp. 1153–1157, China, October 2016.

[7] S. Maresca, P. Braca, J. Horstmann, and R. Grasso, "Maritime surveillance using multiple high-frequency surface-wave radars," *IEEE Transactions on Geoscience and Remote Sensing*, vol. 52, no. 8, pp. 5056–5071, 2014.

[8] K. Saho, "Optimal steady-state range prediction filter for tracking with LFM waveforms," *Applied Sciences (Switzerland)*, vol. 8, Article ID 17, 2018.

[9] M. A. Murzova and V. E. Farber, "The α-β Filter for Tracking Maneuvering Objects with LFM Waveforms," in *Proceedings of the 2017 IVth International Conference on Engineering and Telecommunication (EnT)*, pp. 104–107, November 2017.

[10] J. Vineet and W. D. Blair, "Filter design for steady-state tracking of maneuvering targets with LFM waveforms," *IEEE Transactions on Aerospace and Electronic Systems*, vol. 45, pp. 296–300, 2009.

[11] L. Xu, D. Feng, and X. Wang, "Matched-filter properties of linear-frequency-modulation radar signal reflected from a phase-switched screen," *IET Radar, Sonar & Navigation*, vol. 10, no. 2, pp. 318–324, 2016.

[12] Z. Chen, G. Zeng, C. Zhao, and L. Zhang, "A Phase Error Estimation Method for Broad Beam High-Frequency Radar," *IEEE Geoscience and Remote Sensing Letters*, vol. 12, no. 7, pp. 1526–1530, 2015.

[13] S. Maresca, P. Braca, R. Grasso, and J. Horstmann, "The impact of sea state on HF surface-wave radar ship detection and tracking performances," in *Proceedings of the MTS/IEEE OCEANS 2015 - Genova*, pp. 1–5, Italy, May 2015.

[14] Y. Bar-Shalom, "Negative correlation and optimal tracking with doppler measurements," *IEEE Transactions on Aerospace and Electronic Systems*, vol. 37, no. 3, pp. 1117–1120, 2001.

[15] A. Balleri, A. Farina, and A. Benavoli, "Coordination of optimal guidance law and adaptive radiated waveform for interception and rendezvous problems," *IET Radar, Sonar & Navigation*, vol. 11, no. 7, pp. 1132–1139, 2017.

[16] W. Hongyan, Y. Daobin, and W. Yanhong, "Analysis of LFM-waveform Libraries for Cognitive Tracking Maneuvering Targets," in *Proceedings of the MATEC Web of Conferences*, vol. 59, Article ID 07004, 2016.

[17] M. A. Trofimenko and V. E. Farber, "Influence of range-Doppler coupling on the tracking stability of reentering space objects," in *Proceedings of the 2nd International Conference on Engineering and Telecommunication, En and T 2015*, pp. 41–44, Russia, November 2015.

[18] K. Saho and M. Masugi, "Performance Analysis and Design Strategy for a Second-Order, Fixed-Gain, Position-Velocity-Measured (α-β-η-θ) Tracking Filter," *Applied Sciences*, vol. 7, no. 8, p. 758, 2017.

[19] J. Sudano, "The α-β-η-θ tracker with a random acceleration process noise," in *Proceedings of the IEEE 2000 National Aerospace and Electronics Conference. NAECON 2000. Engineering Tomorrow*, pp. 165–171, Dayton, OH, USA, 2000.